Journal of Nuclear Materials 399 (2010) 114–121

Contents lists available at ScienceDirect

Journal of Nuclear Materials

journal homepage: www.elsevier.com/locate/jnucmat

Prediction of swelling of 18Cr10NiTi austenitic steel over a wide range of displacement rates

A.S. Kalchenko [a], V.V. Bryk [a], N.P. Lazarev [a], I.M. Neklyudov [a], V.N. Voyevodin [a], F.A. Garner [b,*]

[a] National Science Center "Kharkov Institute of Physics and Technology", 61108 Kharkov, Ukraine
[b] Radiation Effects Consulting, Richland, WA 99354, USA

ARTICLE INFO

Article history:
Received 27 September 2009
Accepted 17 January 2010

ABSTRACT

The internal components of pressurized water reactors of Russian types WWER-440 and WWER-1000 are constructed of annealed 18Cr10NiTi steel, a close analog to AISI 321. Void swelling of the internals is a concern for plant life extension and predictive equations are required to assess the potential of swelling in critical components such as the baffle ring or reflection shield that surrounds the WWER core. The only previously available swelling data for this steel were derived at higher than PWR-relevant displacement rates in the BOR-60 fast reactor. The swelling equation previously developed from these data does not incorporate the effect of displacement rate on swelling.

Using heavy-ion irradiation at very high dpa rates (10^{-2} and 10^{-3} dpa s^{-1}) and doses (5–100 dpa) and coupling the results to available neutron data a swelling equation has been developed that specifically incorporates the effect of dpa rate on void swelling. Experimental results allow description of the swelling peak, the incubation period and the steady-state swelling rate over a wide range of irradiation temperature. For the first time it appears possible to describe both ion and neutron data on this steel within the framework of a single empirical model. Swelling maps constructed from this model permit forecasting of the behavior of the steel in WWERs under the required irradiation conditions, not only at already attained exposure doses, but more importantly to higher dose levels that will be reached following plant life extension.

1. Introduction

Pressurized water reactors (PWRs) of Russian design are designated as WWERs (Water-cooled, Water-moderated Energetic Reactors) or VVERs when using the Russian word for water. Two standard designs operate at either 440 or 1000 Mw thermal energy.

The pressure vessel internals (PVI) of WWER-440 and WWER-1000 reactors were designed to be non-removable structural components with a lifetime equal to that the reactor service life. Currently, the first commercial WWER-440 units are approaching their design lifetime of 30 years. Consideration is now being given to the issue of extending their service life for another 10–15 years. It is of vital importance that the WWER-1000 reactors can be demonstrated to substantiate the PVI design both for the originally-specified and the extended lifetimes, especially with respect to compliance with safe operation requirements. This need calls for data concerning the behavior of PVI materials that are experiencing and will continue to experience high damage levels, especially near-core components such as baffle ring and barrel that surrounds the reactor. A major operational and safety issue arises from the recently observed tendency of this steel and closely related steels to develop void swelling at PWR-relevant conditions.

The void swelling of stainless steels is one of the major factors that were found to limit the lifetime of the internal structural components under fast reactor irradiation conditions [1]. Although it was previously considered that under conditions characteristic of water-cooled reactors that swelling would not occur, Garner and coworkers predicted in 1994 that swelling would most likely occur as a consequence not only of gamma-heating of thick plates but also as a consequence of the lower dpa rate characteristic of PWRs [2]. Soon thereafter it was demonstrated that swelling can indeed occur in light-water-cooled thermal reactors as scientists in the USA, France and Japan observed voids or cavities in PWR-type internal components [3–5]. Voids were also found by Russian specialists in the channel tube of the Rovenskaya WWER-1000 Nuclear Power Plant [6]. It has been found that the cavities observed in the WWER environment appear at substantially lower doses than in higher-flux fast reactors at the same irradiation temperature. Similar observations of voids created in various austenitic steels at unexpectedly low temperatures and doses have been observed in low-flux regions of the BN-350 fast reactor [7–9].

* Corresponding author. Tel.: +1 509 946 5542.
E-mail addresses: kalchenko@kipt.kharkov.ua (A.S. Kalchenko), frank.garner@dslextreme.com (F.A. Garner).

0022-3115/$ - see front matter © 2010 Elsevier B.V. All rights reserved.
doi:10.1016/j.jnucmat.2010.01.010

Even at relatively high dpa rates in the BN-350 fast reactor it has been shown that 18Cr10NiTi steels at temperatures between 335 °C and 360 °C and doses of 75–82 dpa can swell at double digit levels while their plasticity drastically decreases [10]. These observations create concern about a possible mechanism of void-induced failure if the service lives of thermal reactors now in operation are extended.

For an extended service life of 60 years the damage level of austenitic steels used as internals of PWR and WWER reactors can reach or exceed 100 dpa. In this case, it is anticipated that swelling under thermal reactor conditions may cause a strong reduction in the incubation period of swelling and a substantial decrease of the lower swelling temperature boundary due to the low dpa rates occurring in PWR internal components (10^{-8}–10^{-7} dpa s^{-1}). This problem is potentially more significant for the WWER-1000 reactors, whose reflection shield or baffle ring is more complicated in shape and is greater in thickness than that of the plates that form the PWR baffle-former assembly. Owing to intense γ-heating characteristic of water-cooled reactors, this leads to local rises in temperature to as much as 460 °C in the WWER-1000 baffle ring, where not only considerable swelling may occur but large gradients in swelling will develop in response to gradients in both dpa rate and temperature [6].

To develop a predictive equation for WWER swelling it would be best if real reactor components or surveillance specimens were available at WWER-relevant conditions. Since only very limited amounts of such data are available, however, the next best case would be materials irradiated at near-PWR conditions in fast reactors, and some limited data of this type are available. However, in order to accumulate additional data over a range of dpa rates one must turn to charged particle acceleration techniques, which is the path chosen in this experiment in order to augment the limited reactor data available.

In the seventies of the last century, the extrapolation of actual reactor data up to high doses was used to predict swelling when designing fast reactor core elements. This approach makes use of empirical regularities that permit the material swelling to be determined as a function of neutron fluence and temperature, but not usually neutron flux. The method is simple and convenient to use. There have been a number of empirical equation forms for swelling employed by various authors [11–15]. The approach requires only information on the observed behavior of swelling versus fluence and temperature, requiring no detailed understanding of the actual swelling process. However, the empirical approach can be used to test parametric dependencies of various theoretical models as well as to uncover dependencies that were not anticipated.

For the purpose of the current effort the following mathematical relationship for swelling of the 18Cr10NiTi steel was used for wrappers of the BOR-60 fast reactor [16,17]:

$$S = 0.55(D - 67 + 0.1T)\exp(-29 \times 10^{-5}(T - 485)^2), \quad (1)$$

where S is swelling (%), D is the damage dose (dpa) and T is the irradiation temperature (°C). Note that the equation does not explicitly incorporate the effect of dpa rate although the dose rate in the data used to derive this equation varies over the range 0.4–1.4×10^{-6} dpa s^{-1}. Note also that the rate of helium production per dpa in the BOR-60 reactor ranges from only 0.1 to 0.4 appm/dpa, which is very much lower than that produced in a PWR spectrum [2].

This paper derives an empirical expression for swelling, including not only the displacement dose and irradiation temperature, but also the dose rate, with a goal of predicting swelling for the conditions characteristic of both heavy-ion accelerators and nuclear reactors of different types. As noted, however, such development must gloss over the possible role of helium and any possible effect of heat-to-heat variations in composition and starting condition.

2. Materials and experimental techniques

18Cr10NiTi steel in the solution annealed state was used in this study. The composition of this steel is 0.08C, 18.2Cr, 10.4Ni, 0.2Ti, 1.2Mn, 0.3Si, all in wt.%. Specimens in the form of 3 mm diameter disks of 0.2 mm thickness were irradiated with 2 MeV Cr^{+3} ions at the NSC KIPT electrostatic heavy-ion accelerator (ESUVI). The depth distribution of damage was calculated using the SRIM-2006 code [18] as shown in Fig. 1. No helium pre-injection was employed.

The specimens for electron microscopy studies were thinned on both sides, choosing the layer at a depth of 100–200 nm from the incident surface for analysis. The choice of this layer was specified first by the necessity of minimizing the effect of the surface and second to avoid the influence of a high concentration of implanted chromium atoms which exert a chemical effect and also act as injected interstitials which tend to reduce void swelling [19]. The displacement levels reported are associated with this layer and irradiations were conducted to doses ranging from 5 to 100 dpa. The chosen displacement rates (10^{-3} dpa s^{-1} and 10^{-2} dpa s^{-1}) and irradiation temperatures were the major variables in this program. Pairs of specimens were irradiated in good contact with the electrical heater base in a specially fabricated target complex. The temperature was actively controlled within ±5 °C and monitored with a thermocouple fixed to the target base.

The removed layer thickness was determined with both a micro-interferometer and a profilometer to an accuracy of ~3 nm. The final thinning of specimens to thicknesses suitable for TEM examination was performed using standard jet electropolishing in the "Tenupol" device on the unirradiated side with the irradiated side of the specimen coated with a protective varnish film to protect it from etching. The electropolishing conditions were as follows: 70 V voltage, room temperature of electrolyte, electrolyte composition of 80% C_2H_5OH, 10% $HClO_4$, and 10% $C_3H_8O_3$. With appearance of a hole in the specimen, the polishing was stopped. The specimen was removed from the Teflon holder, was washed first in ethyl alcohol and then in acetone until the protective varnish film was dissolved. The final washing was done in ethyl alcohol. Electron-microscopic examination of the specimen was performed with electron microscopes JEM-100CX and JEM-2100.

The swelling value was determined from electron-microscope images using the formula:

$$S = 100\% \cdot \frac{\frac{\pi}{6}\sum_{i=1}^{N} d_i^3}{A \cdot h}, \quad (2)$$

where d_i is the diameter of the i-th void, N is the number of all voids, A is the image area, h is the foil thickness of the specimen area under examination. In swelling calculations the error sources arise from inaccuracies when determining the image magnification (2%), the specimen thickness (10%) and the void diameter (5%). Consequently, the total error in the swelling value should be no more than 20%.

3. Experimental results

The ion-induced temperature dependence of swelling at 50 dpa exhibits a near-bell-shaped appearance and shifts by ~25 °C towards higher temperatures with a change in the dose rate from 10^{-3} dpa s^{-1} to 10^{-2} dpa s^{-1} (Fig. 2). At lower dose rates, an increase in the swelling peak and a broadening of the swelling temperature range takes place. Note that the character of the swelling

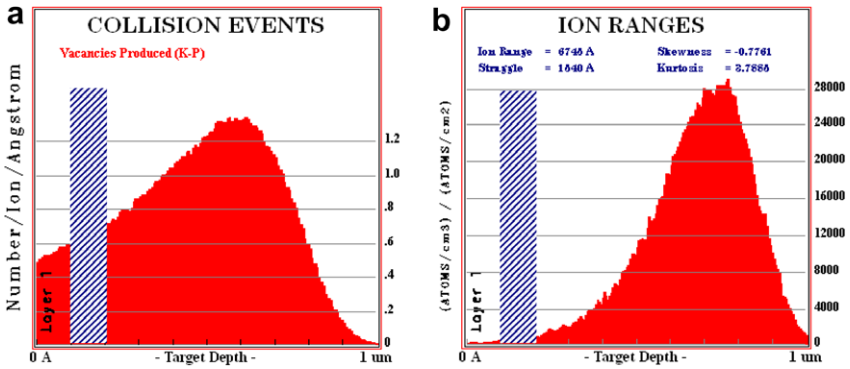

Fig. 1. Profiles of displacement damage (a) and injected ion depth (b) of 2 MeV Cr^{+3} ions computed using the SRIM-2006 code [18] for the 18Cr10NiTi steel. The shaded area shows the depth of the layer under study by microscopy.

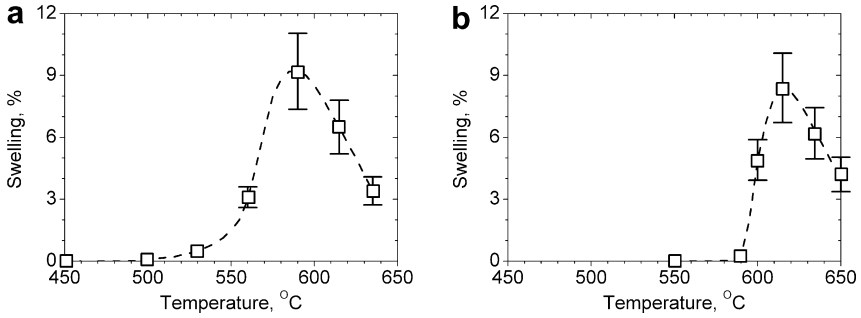

Fig. 2. Swelling versus temperature at an irradiation dose of 50 dpa and dose rates: (a) 1×10^{-3} dpa s^{-1} and (b) 1×10^{-2} dpa s^{-1}.

curve over its rising part (low-temperature swelling range) is more extended at 10^{-3} dpa s^{-1} than at 10^{-2} dpa s^{-1}.

The dose rate effect can also be seen in the volumetric swelling versus displacement dose curves. This effect manifests itself as a change in the incubation dose of swelling, and particularly in the steady-state swelling stage, and it is more pronounced at lower irradiation temperatures (Fig. 3).

4. Development of the modeling function

Based on the data of swelling obtained using heavy-ion irradiation we can construct a fitting function on three parameters: temperature, dose and dose rate. Using heavy-ion irradiation the achievable dose rate varies by only two orders of magnitude, in our case from 10^{-3} to 10^{-2} dpa s^{-1}, and that it is insufficient for an extrapolation to the reactor regime where the dose rate varies from 10^{-8} to 10^{-6} dpa s^{-1}. Fortunately for the steel under consideration there are well-documented data of swelling in the BOR-60 fast reactor (see e.g. [17] and references therein) which can also be incorporated into the development of a fitting function.

The dose dependence in the temperature range close to the peak swelling temperature T_{max} is described as a linear function $S(D) \sim (D - D_0)$ with a some incubation period D_0. This linear dependence of the post-transient swelling rate observed at rather high doses is in good agreement with the theory of void swelling in metals [20]. The linear increase of swelling with dose under neutron irradiation was also observed experimentally by the authors of the empirical Eq. (1) in Refs. [16,17].

Discussion of different definitions of the incubation period D_0 can be found, for example, in Refs. [21,22]. Here the incubation period D_0 is the point of intersection of the tangent to the steady-state swelling curve with the dose axis, as shown in Fig. 4.

As mentioned above, the experimentally observed temperature dependence of swelling $S(T)$ shows a distinct asymmetry (see

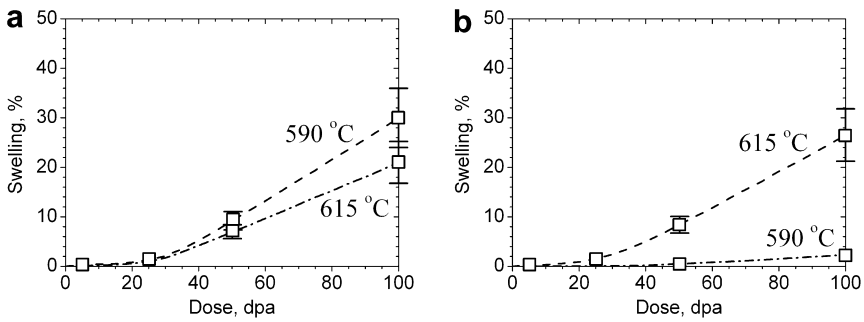

Fig. 3. Dose dependence of swelling at dose rates: (a) 1×10^{-3} dpa s^{-1} and (b) 1×10^{-2} dpa s^{-1}.

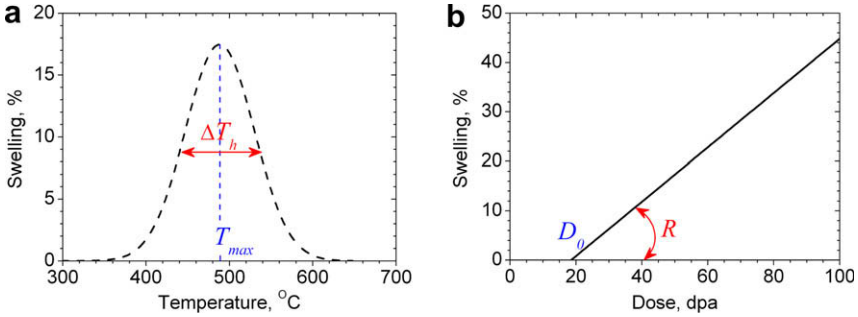

Fig. 4. Schematic representation of swelling dependence on (a) temperature at fixed dose and dose rate; (b) dose at fixed temperature and dose rate. Shown are characteristic values of swelling at a dose of 50 dpa, a dose rate 10^{-6} dpa s^{-1} and a temperature of 590 °C corresponding to fast reactor data taken from [16].

Fig. 2), but for the sake of simplicity, by analogy with Eq. (1), we shall chose the approximating function as a Gaussian distribution in temperature, Fig. 4a,

$$S = R \cdot \varphi(D - D_0) \cdot \exp\left\{-\frac{(T - T_{\max})^2}{2 \cdot \sigma_T^2}\right\}, \quad (3)$$

where S is swelling (%), D is the damaging dose (dpa), D_0 is the incubation period (dpa), T is the irradiation temperature (°C), $T_{\max}$ is the peak swelling temperature (°C), σ_T is the temperature dispersion of the distribution (°C), R is the peak swelling rate at $T = T_{\max}$ (% dpa^{-1}). The function $\phi(x)$ is defined by

$$\varphi(x) = x \cdot \theta(x), \quad \text{where } \theta(x) = 1 \text{ if } x > 0 \text{ and } 0 \text{ if } x \leqslant 0. \quad (3a)$$

Comparison of Eq. (3) with Eq. (1) shows that the incubation period D_0 is in turn the temperature function $D_0(T)$. Furthermore, we assume that R, D_0, $T_{\max}$ and σ_T are functions of the dose rate k.

To obtain the swelling temperature dependence using the functions shown in Figs. 2 and 4a, it is necessary to determine ΔT_h that has a simple geometric interpretation, namely, the full width at half maximum (FWHM). For the Gaussian distribution, ΔT_h is linearly related to σ_T by

$$\sigma_T = \frac{\Delta T_h}{2\sqrt{2\ln 2}}. \quad (4)$$

Let us analyze the experimental swelling curves for this steel measured during irradiation by heavy-ions (Figs. 2 and 3). A more detailed consideration will also be given to the dose–temperature dependence of swelling for the same steel, obtained with the use of the approximating function (1), which was, in its turn, derived on the basis of the experimental fast reactor BOR-60 data. As a matter of convenience the basic experimental data are presented in Table 1 including both heavy-ion accelerator and fast reactor data.

As can be seen from Figs. 2a, b and 4a, the temperature dependence of swelling shows a classic "temperature shift" of the swelling peak towards higher irradiation temperatures with an increase in the dose rate. The maximum temperature of swelling shifts from 490 °C at $k \approx 10^{-6}$ dpa s^{-1} in the reactor irradiation case up to 590 °C at 10^{-3} dpa s^{-1} and to 615 °C at 10^{-2} dpa s^{-1} in the accelerator irradiation cases. Additionally, the distributions differ in width; specifically with an increase in dose rate the temperature dependence of swelling becomes narrower. In our case, to determine the temperature dependence of broadening, we have made use of the above-mentioned concept, viz., FWHM, ΔT_h, a quantity widely used in spectrometry. This quantity can readily be measured by drawing on the temperature curve the straight line parallel to the temperature axis at the half maximum of swelling, and by measuring its length at the intersection of two curves. At dose rates of 10^{-6}, 10^{-3} and 10^{-2} dpa s^{-1} this value was found to be 90, 60 and 50 °C, respectively (see Figs. 2a, b and 4a). After determining ΔT_h, the temperature dispersion σ_T was calculated using relation (4).

Analysis of experimental data on the effect of dose rate k on $T_{\max}(k)$ and $\sigma_T(k)$ presented in Fig. 5 shows that these functions are, within the accuracy of measurements, linear functions of ln k. Therefore, the maximum temperature of swelling $T_{\max}(k)$ and the temperature dispersion $\sigma_T(k)$ can be represented as follows:

$$T_{\max}(k) = 690 + 15.5 \ln k, \quad (5)$$

$$\sigma_T(k) = 12.3 - 1.9 \ln k. \quad (6)$$

Regarding the dose dependence of swelling, the dose rate exerts an effect on both the rate of swelling and the duration of the incubation period. A comparison between the curves shown in Figs. 4b, 3a and b indicates that at the temperatures corresponding to the swelling peaks (490, 590 and 615 °C) the swelling rate at the steady-sate stage declines and is 0.55, 0.4 and 0.35%/dpa, respectively, for 10^{-6}, 10^{-3} and 10^{-2} dpa s^{-1}. In Fig. 6 the approximating function $R(k)$, which has the form:

$$R(k) = 0.25 - 0.022 \ln k, \quad (7)$$

and is plotted as the maximum swelling rate at the steady-state stage versus the dose rate.

Fig. 7a shows the swelling incubation period versus the dose rate and indicates that an increase in dose rate leads to an increase in the incubation period. (The values in Fig. 7a are taken from the curves shown in Figs. 3a, b and 4b.) For the temperatures corresponding to the swelling peak, the incubation period is 18, 27 and 29 dpa for $k \approx 10^{-6}$, 10^{-3} and 10^{-2} dpa s^{-1}, respectively (see the upper value in Figs. 4b, 3a and b). It should be noted that the incubation period is dependent not only on the dose rate, but also on the irradiation temperature. The effect of the irradiation temperature can also be seen in Fig. 7a, where the curves for different irradiation temperatures have the same slope, but shift downwards as the irradiation temperature increases. It should be noted that a similar shortening of the transient regime with increasing temperature was observed in AISI 304 stainless steel irradiated in EBR-II [23].

The approximating functions derived from these data differ only in terms of the derived constants, and account for the influence of temperature. Taking these terms into account (see

Table 1
Selected data on radiation induced swelling of 18Cr10NiTi steel.

k, dpa s^{-1}	$T_{\max}$, °C	ΔT_h, °C	R, %/dpa	D_0^{490}, dpa	D_0^{590}, dpa	D_0^{615}, dpa
10^{-2}	615	50	0.35	n/a	32	29
10^{-3}	590	60	0.4	n/a	27	24
10^{-6} [16]	490	90	0.55	18	8	5.5
10^{-7} [17]	440	n/a	n/a	n/a	n/a	n/a

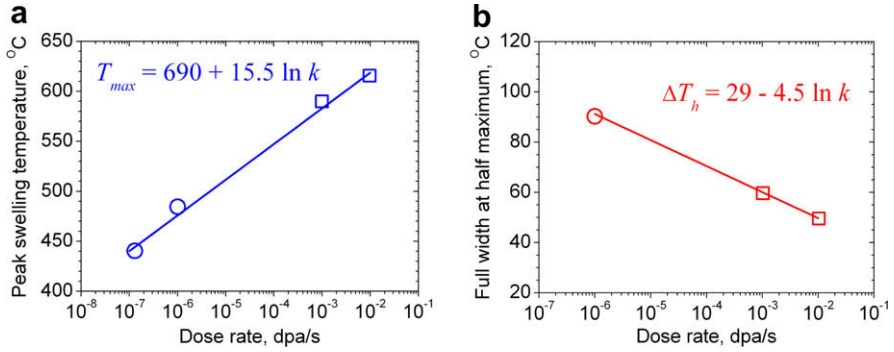

Fig. 5. Peak swelling temperature (a) and temperature distribution (b) versus dose rate in 18Cr10NiTi steel. The symbols ○ and □, respectively, designate the reactor and accelerator data; while the solid lines represent approximations (5) and (6).

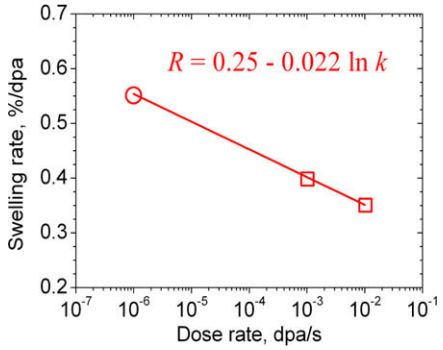

Fig. 6. Peak swelling rate of 18Cr10NiTi steel versus the dose rate.

Fig. 7b), we obtain the incubation period as a function of both the dose rate and the irradiation temperature:

$$D_0(T,k) = 103 - 0.1T + 2.6\ln k. \tag{8}$$

Note the coincidence of the factors that precede the temperature terms in Eqs. (1) and (8).

Substituting all data obtained by the use of Eqs. (5)–(8), namely, the peak swelling temperature $T_{max}(k)$, the temperature dispersion $\sigma_T(k)$, the maximum swelling rate $R(k)$ and the incubation period $D_0(T,k)$ into expression (3), we obtain

$$S = (0.25 - 0.022\ln k)\cdot\varphi(D - 103 + 0.1T - 2.6\ln k) \cdot \exp\left\{-\frac{(T - 690 - 15.5\ln k)^2}{2\cdot(12.3 - 1.9\ln k)^2}\right\}, \tag{9}$$

where S is swelling (%), D is the damaging dose (dpa), T is the irradiation temperature (°C), k is the dose rate (dpa s^{-1}) and the function $\varphi(x)$ is defined by expression (3a).

The use of such empirical equations always invites the question about their validity and accuracy limits. The dose and temperature curves of the 18Cr10NiTi steel swelling, constructed graphically by using expression (9) (Fig. 8), show that the functions $S(D, T, k)$ are in reasonably fair agreement with the experimental data at the temperatures close to the swelling peak and especially at rather high doses.

5. Discussion

Of considerable interest is the effect exerted by the dose rate and the irradiation temperature on the duration of the incubation period D_0. In the current study irradiated 18Cr10NiTi steel exhibits an incubation period that strongly decreases with decreasing dpa rate from 10^{-2} down to 10^{-6} dpa s^{-1}, while it increases with decreasing irradiation temperature (see Figs. 7a and 9). Note that incubation period D_0 at peak swelling temperatures T_{max} increases with dose rate, as shown by the dashed line in Fig. 9. This is in good agreement with the experimental data and theoretical descriptions about the behavior of the incubation period in the temperature range close to the swelling peak in austenitic steels [24,25]. More importantly, the predicted behavior of decreasing incubation period has very clearly been observed in neutron irradiation of very simple Fe–Cr–Ni and Fe–Cr–Ni–Ti model alloys by Okita and coworkers [26,27] and in AISI 304 stainless steel by Garner and coworkers [28,29]. Note that the composition of AISI 304 is very similar to that of 18Cr10NiTi with the primary difference being the absence of titanium.

Another interesting facet of our results is that the post-transient or steady-state swelling rate appears to increase as the dpa rate decreases, a feature also seen in the AISI 304 results of Garner. It is known however that steels that swell rather easily such as AISI 304 and our steel that the swelling rate increases very gradually, prolonging the approach to true steady state behavior. Note that

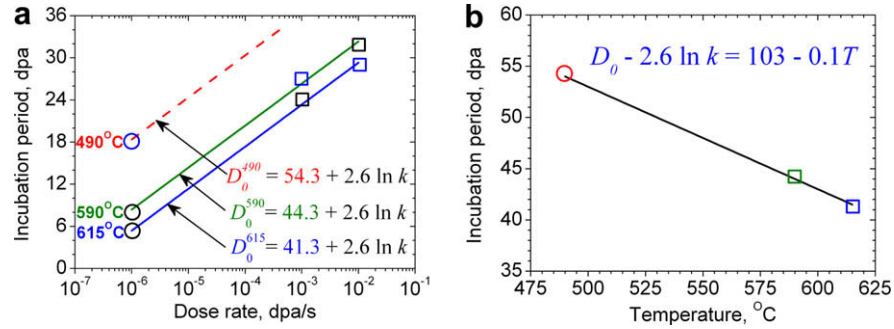

Fig. 7. Incubation period versus dose rate (a) and the coefficient entering into the approximating function versus irradiation temperature (b).

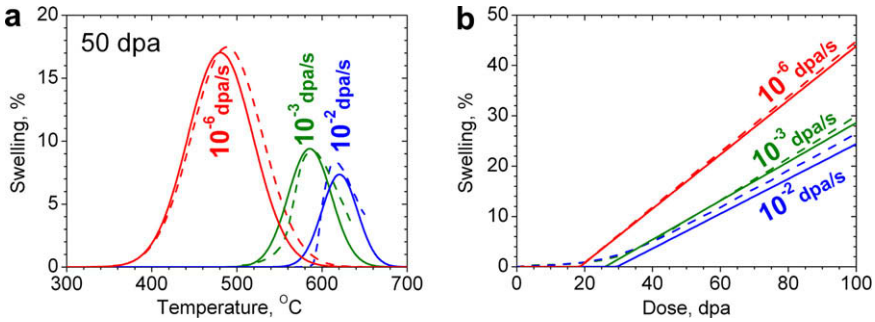

Fig. 8. Comparison between experimental and calculated temperature and dose dependencies of swelling at different dose rates. The dashed lines represent the experimental results and the solid lines are calculations using expression (9).

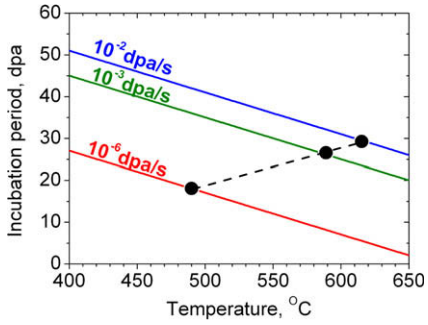

Fig. 9. Incubation period versus irradiation temperature of 18Cr10NiTi steel, calculated by Eq. (8). Filled circles designate the incubation doses at the peak swelling temperatures and the dashed line shows the temperature dependence of $D_0(T_{max})$.

neither the AISI 304 data nor that of our steel have reached the 1%/dpa rate known to be the terminal or maximum steady-state swelling rate of all austenitic stainless steels [1]. In the neutron irradiation work of Okita, however, the transient regime always ended with the model alloys quickly developing a steady-state swelling rate of 1%/dpa.

More importantly, when Okita and coworkers conducted similar tests using nickel ion irradiation on Fe–15Cr–16Ni at three displacement rates between 10^{-4} and 10^{-3} dpa s^{-1} between 300 and 600 °C, they showed not only that the incubation dose increased with increasing dpa rate but that the post-transient swelling rate also appeared to fall with increasing dpa rate [30]. It is not clear at this point if ion-induced swelling at very high dpa rates precludes attainment of the terminal rate of 1%/dpa or merely prolongs its attainment to much higher doses. Okita's various works do show, however, that the transition between the transient and steady-state regimes in simple ternary or quaternary alloys is related primarily to the dpa rate-dependent shift from loop-dominated to line-dominated dislocation microstructures, and that in his ion studies the loop-dominant phase persists to much higher doses, precluding the onset of the higher steady-state swelling rate.

Fig. 10 shows predicted dose–temperature maps of 18Cr10NiTi swelling that were calculated using expression (9) at different dose rates typical of accelerator irradiation ($k = 10^{-3}$ dpa s^{-1}), fast reactor ($k = 10^{-6}$ dpa s^{-1}) and low-flux thermal reactor ($k = 10^{-8}$ dpa s^{-1}) environments. The swelling becomes progressively larger at lower dpa rates. The generality of this phenomenon is supported by other studies on a variety of austenitic steels, such as that of Budylkin and coworkers [31] and Seran and Dupouy [32]. In every case the shortened incubation period at lower dpa rates leads to earlier and therefore more swelling at the lower dpa rates. In one exceptional study the 18Cr10NiTi steel when irradiated in the BR-10 fast reactor at a very low dpa rate (1.9×10^{-9} dpa s^{-1}) was observed at 350 °C to be clearly swelling after accumulating only 0.6 dpa [33].

As seen in Fig. 10, with increasing dose rate at a given dose the temperature corresponding to the swelling peak shifts towards higher temperatures. This temperature "shift" is known to be due to the necessity of keeping constant the relationship between the rates of point defect formation and disappearance at sinks so that the vacancy supersaturation level characteristic of charged particle irradiation conditions should be maintained at reactor-relevant levels [20].

Note that with a decrease in dose rate the void swelling at the maximum ($T_{max} = 590$ °C at 10^{-3} dpa s^{-1} against 490 °C at 10^{-6} dpa s^{-1}) increases from 9.35% up to 16.9% at 50 dpa. Based on the treatment presented in [33] it is assumed that such behavior of swelling is due to a decrease in the rate of point defect recombination, and hence, the increase in the number of vacancies that reach the void as the dose rate decreases. Consequently, a further reduction in the rate of atomic displacement should lead to additional increase of void swelling. Note that swelling under thermal reactor irradiation conditions is expected to be greater as demonstrated in Fig. 10c ($S = 23.1\%$ at $T_{max} = 404$ °C, 50 dpa, 10^{-8} dpa s^{-1}). One consequence of these results is that while the original equation swelling equation developed for this steel from BOR-60 results would predict rather significant swelling in the baffle ring of a WWER-1000 [17], our dpa rate-dependent equation will predict much more swelling.

As mentioned above, with decreasing dose rate the temperature dependence of swelling gets wider (Fig. 5b). This effect manifests itself in the widening of the temperature range of swelling (cf. Fig. 10a–c). The behavior of the lower temperature range of threshold formation is similar to that of the swelling peak temperature, i.e., it shifts to the higher irradiation temperature region with increased dose rate. At lower dose rates, the incubation period becomes shorter (e.g., for 590 °C we have $D_0 = 32$, 27 and 8 dpa at 10^{-2}, 10^{-3} and 10^{-6} dpa s^{-1}, respectively, see Fig. 7a), and swelling develops at much lower temperatures and doses as observed in earlier referenced studies, and therefore the temperature regime of swelling extends strongly towards lower irradiation temperatures.

The present results demonstrate that with due attention for dose rate scaling the basic physical processes involved in the swelling phenomenon occur under both heavy-ion and fast reactor irradiation conditions in a very general manner. Apparently, the influence of the very low levels of helium produced in the BOR-60 fast reactor (0.1–0.4 appm/dpa) is not a strongly governing consideration, at least in this easily swelling steel. At the same time, the production of helium and hydrogen in the internals of WWER-type and PWR-type thermal reactors for 30 years of their service exceeds 1000 and 2000 appm, correspondingly [2,34,35]. These high gas concentrations may substantially change the

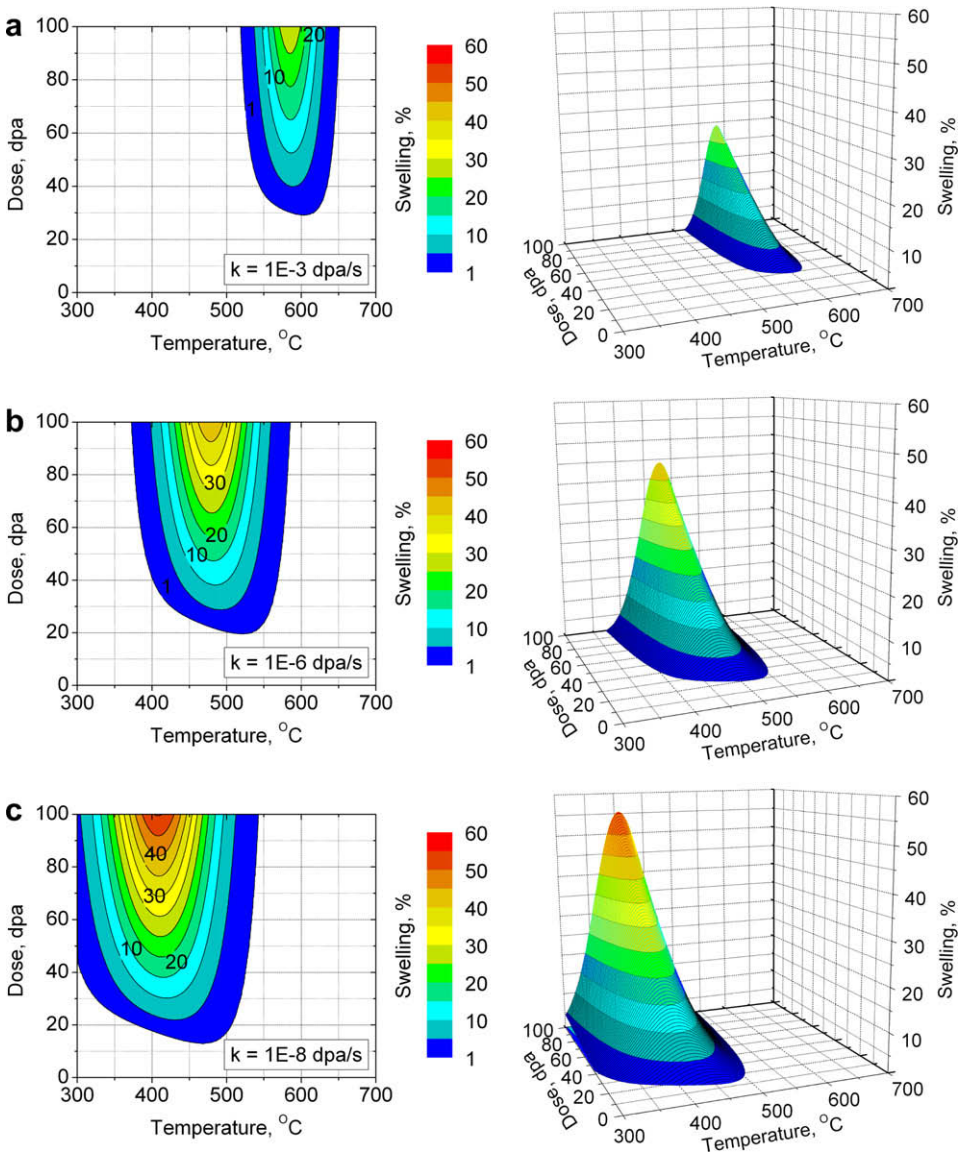

Fig. 10. Temperature–dose maps of 18Cr10NiTi steel swelling for different dose rates [(a) 10^{-3} dpa s^{-1}, (b) 10^{-6} dpa s^{-1}, (c) 10^{-8} dpa s^{-1}], calculated by the fitting function (expression 9).

character of void nucleation and structural-phase transformations. In this regard, it appears that it might be necessary to include the rate of gas production as an additional parameter into the modeling function. Investigation is now ongoing to determine experimentally the effects of high gas generation rates on the swelling of this steel.

6. Conclusions

An empirical equation incorporating both ion bombardment and fast reactor data on annealed 18Cr10NiTi steel has been developed to provide prediction of void swelling anticipated in the austenitic core internal components of WWER reactors, especially under conditions expected due to plant life extension. This equation explicitly contains a dependence not only on the dpa level and irradiation temperature but also the dpa rate, an approach not normally taken in earlier studies that produced equations containing no dose rate dependence.

Employing simulation by heavy-ion irradiation it has been demonstrated that with a decrease in dose rate toward levels characteristic of WWERs the temperature regime of swelling for 18Cr10NiTi steel will get broader and show a shift of the swelling peak toward lower temperatures. Increased swelling at lower dpa rates develops primarily from a decrease in the incubation period of swelling and an apparent increase in the post-transient swelling rate. Increases in irradiation temperature were also found to decrease the post-transient swelling rate. These results agree with the results of other neutron irradiation studies on this steel and other austenitic steels.

On the basis of the developed empirical equation relatively large levels of swelling are anticipated to occur in the WWER baffle ring, especially at dose levels to be reached following plant life extension. Such information is crucial in making decisions concerning extended operation of WWERs, with or without replacement of the internals.

Acknowledgement

The authors express their special gratitude to V.V. Melnichenko for irradiating specimens at the ESUVI accelerator.

References

[1] F.A. Garner, Chapter 6: irradiation performance of cladding and structural steels in liquid metal reactors, Vol. 10A of Materials Science and Technology: A Comprehensive Treatment, VCH Publishers, 1994, pp. 419–543.
[2] F.A. Garner, L.R. Greenwood, D.L. Harrod, Potential high fluence response of pressure vessel internals constructed from austenitic stainless steels, in: R.E. Gold, E.P. Simonen (Eds.), Sixth International Symposium on Environmental Degradation of Materials in Nuclear Power Systems – Water Reactors, The Minerals, Metals and Materials Society, 1993, pp. 783–790.
[3] J. Edwards, E.P. Simonen, F.A. Garner, L.R. Greenwood, B.M. Oliver, S.M. Bruemmer, J. Nucl. Mater. 317 (2003) 32–45.
[4] K. Fujii, K. Fukuya, G. Furutani, T. Torimaru, A. Kohyama, Y. Katoh, Swelling in 316 stainless steel irradiated to 53 dpa in a PWR, in: 10th International Symposium on Environmental Degradation of Materials in Nuclear Power Systems – Water Reactors, The Minerals, Metals and Materials Society, Pennsylvania (2002) CD format.
[5] C. Pokor, Y. Thebault, J.-P. Massoud, M. Delnondedieu, D. Loisnard, E. Lemaire, N. Ligneau, P. Dubuisson, J. Kocik, E. Keilova, Microstructural evolution of neutron irradiated stainless steels: comparison between irradiations in experimental reactors and in pressurized water reactors, in: Fontevraud-6 Symposium on Contribution of Materials Investigations to Improve the Safety and Performance of LWRs, 18–22 September 2006, Fontevraud, France, pp. 637–648.
[6] V.S. Neustroev, V.G. Dvoretsky, Z.E. Ostrovsky, V.K. Shamardin, G.A. Shimansky, Studies into the microstructure and mechanical properties of 18Cr10NiTi steel after irradiation in the WWER-1000 Core, in: Problems of Atomic Science and Technology- Series: Radiation Damage Physics and Radiation Materials Science, 2003, vol. 3 (83), pp. 73–78 (in Russian).
[7] F.A. Garner, S.I. Porollo, Yu.V. Konobeev, V.S. Neustroev, O.P. Maksimkin, Void swelling of russian austenitic stainless steels at PWR-relevant displacement rates and temperatures, in: Fontevraud-6 Symposium on Contribution of Materials Investigations to Improve the Safety and Performance of LWRs, 18–22 September 2006, Fontevraud, France, pp. 637–648.
[8] O.P. Maksimkin, K.V. Tsai, L.G. Turubarova, T. Doronina, F.A. Garner, J. Nucl. Mater. 329–333 (2004) 625–629.
[9] O.P. Maksimkin, K.V. Tsai, L.G. Turubarova, T.A. Doronina, F.A. Garner, J. Nucl. Mater. 367–370 (2007) 990–994.
[10] S.I. Porollo, A.N. Vorobjev, Yu.V. Konobeev, A.M. Dvoriashin, V.M. Krigan, N.I. Budylkin, E.G. Mironova, F.A. Garner, J. Nucl. Mater. 258–263 (1998) 1613–1617.
[11] V.N. Bykov, V.D. Dmitriev, L.G. Kostromin, Atomnaya Energy. 40 (4) (1976) 293–295 (in Russian).
[12] S. Oldberg, D. Sandusky, P.L. Schaboy, E.A. Compretly, Trans. Amer. Nucl. Soc. 12 (2) (1969) 588–589.
[13] A. Boltax, P. Murray, A. Biancheria, Nucl. Appl. Tech. 9 (1970) 326–337.
[14] F.A. Garner, J.J. Laidler, G.L. Guthrie, Development and evaluation of a stress-free swelling correlation for 20% cold-worked 316 stainless steel, in: Irradiation Effect on the Microstructure and Properties of Metals, ASTM STP 611, 1976, pp. 208–276.
[15] J.P. Foster, R.V. Strain, Nucl. Tech. 24 (1974) 93–98.
[16] S.N. Votinov, V.I. Prokhorov, Z.E. Ostrovsky, Irradiated stainless steels, Nauka publ. (1987), 128.
[17] V.S. Neustroev, V.K. Shamardin, Z.E. Ostrovsky, A.M. Pecherin, F.A. Gamer, Temperature-shift of void swelling observed in annealed Fe–18Cr–10Ni–Ti stainless steel irradiated in the reflector region of BOR-60, in: Effects of Radiation on Materials: 19th Symposium, ASTM STP 1366, 2000, pp. 792–800.
[18] J.P. Biersack, L.G. Haggmark, Nucl. Instrum. Meth. 174 (1980) 257–269.
[19] F.A. Garner, J. Nucl. Mater. 117 (1983) 177–197.
[20] L.K. Mansur, Nucl. Technol. 40 (1978) 5–34.
[21] V.F. Zelensky, I.M. Neklyudov, T.P. Chernyaeva, Naukova Dumka (1988) 296 (in Russian).
[22] V.N. Voyevodin, I.M. Neklyudov, Naukova Dumka (2006) 376 (in Russian).
[23] F.A. Garner, D.L. Porter, A reassessment of the swelling behavior of AISI 304L stainless steel, in: Proceedings International Conference on Dimensional Stability and Mechanical Behavior of Irradiated Metals and Alloys, April 11–13, 1983, Brighton, England, vol. II, pp. 41–44.
[24] F.A. Garner, M.B. Toloczko, B.H. Sencer, J. Nucl. Mater. 276 (2000) 123–142.
[25] M.P. Surh, J.B. Sturgeon, W.G. Wolfer, J. Nucl. Mater. 328 (2004) 107–114.
[26] T. Okita, N. Sekimura, F.A. Garner, L.R. Greenwood, W.G. Wolfer and Y. Isobe, Neutron-induced microstructural evolution of Fe–15Cr–16Ni alloys at $\sim$ 400 °C during neutron irradiation in the FFTF fast reactor, in: 10th International Conference on Environmental Degradation of Materials in Nuclear Power Systems – Water Reactors, 2001, issued on CD format.
[27] T. Okita, N. Sekimura, T. Sato, F.A. Garner, L.R. Greenwood, J. Nucl. Mater. 307–311 (2002) 322–326.
[28] G.M. Bond, B.H. Sencer, F.A. Garner, M.L. Hamilton, T.R. Allen, D.L. Porter, Void swelling of annealed 304 stainless steel at $\sim$370–385 °C and PWR-relevant displacement rates, in: 9th International Conference on Environmental Degradation of Materials in Nuclear Power Systems – Water Reactors, 1999, pp. 1045–1050.
[29] F.A. Garner, B.J. Makenas, Recent experimental results on neutron-induced void swelling of AISI 304 stainless steel concerning its interactive dependence on temperature and displacement rate, in: Fontevraud-6 Symposium on Contribution of Materials Investigations to Improve the Safety and Performance of LWRs, 18–22 September 2006, Fontevraud, France, pp. 625–626.
[30] N.I. Budylkin, T.M. Bulanova, E.G. Mironova, N.M. Mitrofanova, S.I. Porollo, V.M. Chernov, V.K. Shamardin, F.A. Garner, J. Nucl. Mater. 329–333 (2004) 621–624.
[31] J.L. Seran, J.M. Dupouy, The swelling of solution annealed 316 cladding in Rapsodie and Phenix, in: Effects of Radiation on Materials: 11th Int. Symp., ASTM STP 782, 1982, pp. 5–16.
[32] T. Okita, T. Sato, N. Sekimura, T. Iwai, F.A. Garner, J. Nucl. Mater. 367–370 (2007) 930–934.
[33] I. Porollo, A.M. Dvoriashin, Yu.V. Konobeev, A.A. Ivanov, S.V. Shulepin, F.A. Garner, J. Nucl. Mater. 359 (2006) 41–49.
[34] F.A. Garner, E.P. Simonen, B.M. Oliver, L.R. Greenwood, M.L. Grossbeck, W.G. Wolfer, P.M. Scott, J. Nucl. Mater. 356 (2006) 122–135.
[35] D.J. Edwards, F.A. Garner, S.M. Bruemmer, P. Efsing, J. Nucl. Mater. 384 (2009) 249–255.